Predictions on $B \to \pi \bar{l} \nu_l$, $D \to \pi \bar{l} \nu_l$, and $D \to K \bar{l} \nu_l$ from QCD light-cone sum rules

A. Khodjamirian,[1,2,*] R. Rückl,[2] S. Weinzierl,[3] C. W. Winhart,[2] and O. Yakovlev[2,4]

[1]*The Niels Bohr Institute, DK-2100 Copenhagen, Denmark*
[2]*Institut für Theoretische Physik, Universität Würzburg, D-97074 Würzburg, Germany*
[3]*NIKHEF, P.O. Box 41882, 1009-DB Amsterdam, The Netherlands*
[4]*Randall Laboratory of Physics, University of Michigan, Ann Arbor, Michigan 48109-1120*

The f^+ form factors of the $B \to \pi$, $D \to \pi$ and $D \to K$ transitions are calculated from QCD light-cone sum rules (LCSRs) and used to predict the widths and differential distributions of the exclusive semileptonic decays $B \to \pi \bar{l} \nu_l$, $D \to \pi \bar{l} \nu_l$ and $D \to K \bar{l} \nu_l$, where $l = e, \mu$. The current theoretical uncertainties are estimated. The LCSR results are found to agree with the results of lattice QCD calculations and with experimental data on exclusive semileptonic D decays. Comparison of the LCSR prediction of $B \to \pi \bar{l} \nu_l$ with the CLEO measurement yields a value of $|V_{ub}|$ in agreement with other determinations.

PACS number(s): 12.38.Lg, 11.55.Hx, 13.20.Fc, 13.20.He

I. INTRODUCTION

The measurement of the exclusive semileptonic decay $B \to \pi \bar{l} \nu_l$ by the CLEO Collaboration [1] can be used to determine the Cabibbo-Kobayashi-Maskawa (CKM) parameter $|V_{ub}|$. This exclusive method provides an important alternative to the extraction of $|V_{ub}|$ from inclusive measurements of $B \to X_u \bar{l} \nu_l$. However, it requires a reliable calculation of the form factor $f^+_{B\pi}(p^2)$ defined by

$$\langle \pi(q)|\bar{b} \gamma_\mu u|B(p+q)\rangle$$
$$= 2 f^+_{B\pi}(p^2) q_\mu + [f^+_{B\pi}(p^2) + f^-_{B\pi}(p^2)] p_\mu, \quad (1)$$

q and $p+q$ being the π- and B-meson four-momenta, respectively. In the case of semileptonic decays into the light leptons $l = e, \mu$, the form factor $f^-_{B\pi}(p^2)$ plays a negligible role. A particularly promising approach to evaluate $f^+_{B\pi}(p^2)$ is based on QCD light-cone sum rules (LCSRs) [2] which combine operator product expansion (OPE) on the light cone [3–5] with QCD sum rule techniques [6]. The twist 2, 3 and 4 contributions to the LCSRs for $f^+_{B\pi}(p^2)$ in leading order in α_s have been derived in Refs. [7,8], while the next-to-leading order corrections to the twist 2 term have been calculated in Refs. [9–11]. The LCSR technique has further been applied to $B \to K$ [7,12], $D \to \pi$ [8,11], and $D \to K$ [13] transition form factors.

In this paper we update and improve the predictions of the decay distributions and integrated widths for $B \to \pi \bar{l} \nu_l$, $D \to \pi \bar{l} \nu_l$ and $D \to K \bar{l} \nu_l$. In particular, we include the twist 2 next-to-leading order (NLO) α_s corrections into the calculation of the form factors $f^+_{D\pi}$ and f^+_{DK}. Moreover, we reanalyze the momentum dependence of the form factors. The LCSR for $f^+(p^2)$ is valid at small and intermediate momentum transfer squared

$$p^2 \leqslant m^2_Q - 2 m_Q \chi, \quad (2)$$

where χ is a typical hadronic scale of roughly 500 MeV and independent of the heavy quark mass m_Q. In order to go beyond this limit, we use a second LCSR for the residue of the pole contribution from the ground-state vector mesons B^*, D^* and D^*_s, respectively, which are expected to dominate at large p^2. Previously, we interpolated between the LCSR prediction at small p^2 and the single-pole approximation at large p^2 using a simple, but physically not very intuitive parametrization. In the present paper, we follow a different philosophy. We use the general dispersion relation for the form factor $f^+(p^2)$ and model the integral over the excited vector meson states by an effective pole. This yields a two-pole representation of f^+ as suggested recently in Ref. [14]. The parameters of this representation are determined from the two light-cone sum rules. This approach is more physical and has the benefit of making eventual effects from excited vector meson states more transparent. Finally, we discuss the sources of theoretical uncertainties of the LCSR method one by one, and give a careful estimate of the present overall uncertainty.

Wherever possible, we compare our results with the latest lattice data. From $B \to \pi \bar{l} \nu_l$, the CKM-matrix element $|V_{ub}|$ is determined by comparing the LCSRs and experimental widths. Conversely, the LCSR method is tested using the experimental widths of $D \to \pi \bar{l} \nu_l$ and $D \to K \bar{l} \nu_l$ and the known values of $|V_{cd}|$ and $|V_{cs}|$, respectively. This analysis favors a value m_s (1 GeV) ≈ 150 MeV for the s-quark mass.

The paper is organized as follows. Sections II and III are devoted to the $B \to \pi$ transition as a prototype example. In Sec. II we present the LCSR analysis of $f^+_{B\pi}(p^2)$, the theoretical uncertainties of which are estimated and discussed in Sec. III. The analogous analysis of the $D \to \pi$ and $D \to K$ transitions is described in Sec. IV. Section V deals with applications to decay distributions and integrated widths for $B \to \pi \bar{l} \nu_l$, $D \to \pi \bar{l} \nu_l$ and $D \to K \bar{l} \nu_l$. This section also summarizes the comparison of theory with experiment.

---

*On leave from Yerevan Physics Institute, 375036 Yerevan, Armenia.

II. THE FORM FACTOR $F_{B\pi}^+(P^2)$

The LCSR for the form factor $f_{B\pi}^+(p^2)$ is obtained from the correlation function

$$F_\mu(p,q) = i \int dx e^{ip \cdot x}$$

$$\times \langle \pi(q) | T\{\bar{u}(x)\gamma_\mu b(x), m_b \bar{b}(0) i \gamma_5 d(0)\} | 0 \rangle$$

(3)

by contracting the b-quark fields in the time-ordered product of currents, expanding the remaining matrix elements of non-local operators in terms of light-cone distribution amplitudes of the pion, and writing a dispersion relation in the $B(\bar{b}d)$ channel. The derivation is described in detail in Refs. [7–9,15]. Schematically, the resulting sum rule has the form

$$f_{B\pi}^+(p^2) = \frac{1}{2m_B^2 f_B} \exp\left(\frac{m_B^2}{M^2}\right) \left[F_0^{(2)}(p^2, M^2, m_b^2, s_0^B, \mu_b) \right.$$

$$+ \frac{\alpha_s(\mu_b)}{3\pi} F_1^{(2)}(p^2, M^2, m_b^2, s_0^B, \mu_b)$$

$$\left. + F_0^{(3,4)}(p^2, M^2, m_b^2, s_0^B, \mu_b) \right],$$

(4)

where m_B is the B-meson mass, m_b the b-quark pole mass, and f_B the B-meson decay constant defined by the matrix element

$$\langle 0 | m_b \bar{q} i \gamma_5 b | B \rangle = m_B^2 f_B .$$

(5)

The mass scale M is associated with a Borel transformation usually performed in sum rule calculations. It characterizes the off-shellness of the b quark. The scale μ_b is the factorization scale separating soft and hard dynamics. Long-distance effects involving scales lower than μ_b are absorbed in the pion distribution amplitudes which represent the universal nonperturbative input in LCSRs. They have been studied up to twist 4 and are given in Refs. [8,15,16]. The short-distance effects are incorporated in hard-scattering amplitudes calculated perturbatively and convoluted with the pion distribution amplitudes. The first two terms in the brackets in Eq. (4) represent the NLO twist 2 contributions, while the third term refers to the twist 3 and 4 contributions which are only known in LO. For illustration, the leading term $F_0^{(2)}$ is given by

$$F_0^{(2)}(p^2, M^2, m_b^2, s_0^B, \mu_b)$$

$$= m_b^2 f_\pi \int_\Delta^1 \frac{du}{u} \exp\left(-\frac{m_b^2 - p^2(1-u)}{uM^2} \right) \varphi_\pi(u, \mu_b)$$

(6)

with $f_\pi = 132$ MeV being the decay constant and φ_π being the twist 2 distribution amplitude of the pion. The latter can be interpreted as the probability amplitude for finding a quark with momentum fraction u inside a pion. The lower
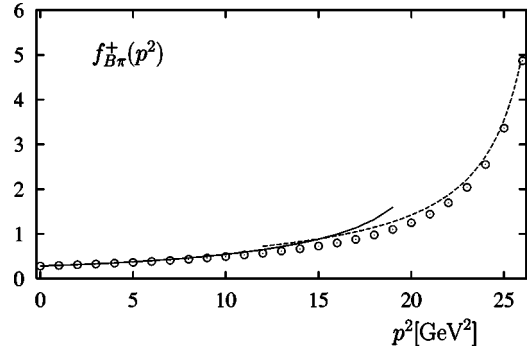

FIG. 1. The $B \rightarrow \pi$ form factor: direct LCSR prediction (solid curve), B^*-pole contribution with the LCSR estimate of the residue (dashed curve), and two-pole parametrization (19) (circles).

integration boundary $\Delta = (m_b^2 - p^2)/(s_0^B - p^2)$ is determined by the effective threshold parameter s_0^B which originates from the subtraction of excited resonances and continuum states contributing to the dispersion integral in the B channel. This subtraction is performed assuming quark-hadron duality at $(p+q)^2 \geq s_0^B$. The explicit expressions for the remaining terms $F_1^{(2)}$ and $F_0^{(3,4)}$ can be found in Refs. [9,10] and Refs. [7,8], respectively.

Numerically, we take $f_B = 180 \pm 30$ MeV, $m_b = 4.7 \mp 0.1$ GeV, $s_0^B = 35 \pm 2$ GeV^2, and $\mu_b = \sqrt{m_B^2 - m_b^2} \approx 2.4$ GeV. Here and in forthcoming theoretical results, the error notation is to be interpreted as a range reflecting the present theoretical uncertainty, e.g., $f_B = 150$–210 MeV. It is also important to note that the above parameters are interrelated by the two-point QCD sum rule for f_B [17]. Consequently, their variation within the given ranges is correlated as indicated by the alternating $\pm$ signs. Furthermore, sum rules for observables should in principle be independent of the auxiliary Borel parameter M^2. In practice, however, this is not the case because of the various approximations made. The allowed range of M^2 differs for different sum rules. For LCSRs it is usually determined by requiring the twist 4 contribution not to exceed 10% and the contributions from excited and continuum states to stay below 30%. Specifically, for the sum rule (4), these criteria yield $M^2 = 10 \pm 2$ GeV^2. In the case of the two-point sum rule for f_B, the allowed interval of the Borel parameter is $M^2 = 4 \pm 2$ GeV^2. With the nominal values of the parameters specified above the LCSR (4) leads to the form factor $f_{B\pi}^+(p^2)$ shown by the solid curve in Fig. 1. In particular, at $p^2 = 0$ one gets

$$f_{B\pi}^+(0) = 0.28 \pm 0.05.$$

(7)

The estimate of the theoretical uncertainty will be explained in detail in the following section.

As already mentioned in the Introduction, the LCSR (4) is expected to hold only at $p^2 \lesssim m_b^2 - 2m_b\chi \approx 18$ GeV^2. Indeed, at $p^2 > 20$ GeV^2 the twist 4 contribution is found to grow strongly, and the stability of the sum rule against variation of the Borel parameter M^2 is lost. This clearly signals the breakdown of the light-cone expansion. On the other hand, as p^2 approaches the kinematical limit $(m_B - m_\pi)^2$ the

lowest-lying B^* pole is expected to give the dominant contribution to $f^+_{B\pi}$. The residue of this pole contribution is given by the product of the B^* decay constant defined by

$$\langle 0 | \bar{q} \gamma_\mu b | B^* \rangle = m_{B*} f_{B*} \epsilon_\mu \qquad (8)$$

and the strong $B^* B \pi$ coupling constant defined by

$$\langle \bar{B}^{*0} \pi^- | B^- \rangle = -g_{B*B\pi}(q \cdot \epsilon). \qquad (9)$$

This product can be calculated from another LCSR which follows from the same correlation function (3) as the LCSR (4), considering this time, however, a double dispersion relation in the B and B^* channel. Again, we only indicate the schematic form of this sum rule [8,11]:

$$f_{B*} g_{B*B\pi} = \frac{1}{m_B^2 m_{B*} f_B} e^{(m_B^2 + m_{B*}^2)/2M^2} \left[G_0^{(2)}(M^2, m_b^2, s_0^B, \mu_b) \right.$$

$$+ \frac{\alpha_s(\mu_b)}{3\pi} G_1^{(2)}(M^2, m_b^2, s_0^B, \mu_b)$$

$$\left. + G_0^{(3,4)}(M^2, m_b^2, s_0^B, \mu_b) \right]. \qquad (10)$$

In analogy to Eq. (4), the NLO twist 2 contributions are denoted by $G_0^{(2)}$ and $G_1^{(2)}$, while $G_0^{(3,4)}$ stands for the LO twist 3 and 4 contribution. Explicitly, the leading twist 2 term is given by

$$G_0^{(2)}(M^2, m_b^2, s_0^B, \mu_b)$$

$$= m_b^2 M^2 (e^{-m_b^2/M^2} - e^{-s_0^B/M^2}) f_\pi \varphi_\pi(u_0, \mu_b). \qquad (11)$$

In contrast to Eq. (6) where one has an integral over the normalized distribution amplitude φ_π, the above term depends on the value of φ_π at the point $u_0 \approx 0.5$. This difference also applies to terms of higher twist, whence the LCSR (10) is much more sensitive to the precise shape of the pion distribution amplitudes than the LCSR (4). The parameters of the two LCSR coincide with the exception of the Borel mass which in the case of Eq. (10) is constrained to the interval $M^2 = 9 \pm 3$ GeV^2. Numerically, we obtain [11]

$$f_{B*} g_{B*B\pi} = 4.4 \pm 1.3 \text{ GeV.} \qquad (12)$$

Again, the uncertainty estimate will be discussed in the next section.

In order to determine the form factor $f^+_{B\pi}(p^2)$ at large momentum transfers $p^2 > 18$ GeV^2, where we cannot rely on the LCSR (4), we consider the dispersion relation

$$f^+_{B\pi}(p^2) = \frac{f_{B*} g_{B*B\pi}}{2m_{B*}(1 - p^2/m_{B*}^2)} + \int_{s_0}^{\infty} \frac{d\tau \rho(\tau)}{\tau - p^2}. \qquad (13)$$

Here, the pole term is due to the ground state B^* meson and the dispersive integral takes into account contributions from higher resonances and continuum states in the B^* channel.

Using Eq. (12), the B^*-pole contribution is shown by the dashed curve in Fig. 1. With decreasing momentum transfer the one-pole approximation deviates noticeably from the LCSR result (4). At $p^2 = 0$ the difference reaches about 50%, showing that the dispersion integral in Eq. (13) over the heavier states cannot be neglected. In Ref. [14], it has been suggested to model their contribution by an effective second pole:

$$f^+_{B\pi}(p^2) = c_B \left(\frac{1}{1 - p^2/m_{B*}^2} - \frac{\alpha_{B\pi}}{1 - p^2/\gamma_{B\pi} m_{B*}^2} \right). \qquad (14)$$

By means of the LCSRs (4) and (10) one can now determine the parameters c_B and $\alpha_{B\pi}$. From Eqs. (12) and (13) we get

$$c_B = \frac{f_{B*} g_{B*B\pi}}{2m_{B*}} = 0.41 \pm 0.12, \qquad (15)$$

and putting $p^2 = 0$ in Eq. (14) and using directly Eqs. (4) and (10) we obtain

$$\alpha_{B\pi} = 1 - \frac{2m_{B*} f^+_{B\pi}(0)}{f_{B*} g_{B*B\pi}} = 0.32^{+0.21}_{-0.07}. \qquad (16)$$

It should be emphasized that the latter result is independent of f_B or the corresponding two-point sum rule. Moreover, since the LCSRs (4) and (10) involve common parameters, some of the uncertainties cancel in the ratio (16). In the heavy quark limit [15], $f^+_{B\pi}(0)$ should scale like $1/m_b^{3/2}$ which implies a positive sign for $\alpha_{B\pi}$. Thus, the result (16) nicely demonstrates the consistency of the LCSR method with the heavy quark limit. The remaining parameter $\gamma_{B\pi}$ can in principle be obtained by fitting Eq. (14) to Eq. (4) at $p^2 < 15$ GeV^2 with c_B and $\alpha_{B\pi}$ fixed. However, since the LCSR prediction deviates in shape very little from the B^*-pole contribution as can be anticipated from Fig. 1, the fit only gives the lower bound $\gamma_{B\pi} > 2$.

In the combined limit $m_Q \to \infty$ and $E_\pi \to \infty$, one has a relation between $f^+_{B\pi}$ and the scalar form factor

$$f^0_{B\pi}(p^2) = f^+_{B\pi}(p^2) + \frac{p^2}{m_B^2 - m_\pi^2} f^-_{B\pi}(p^2), \qquad (17)$$

namely [18]

$$f^0_{B\pi} = \frac{2E_\pi}{m_B} f^+_{B\pi}. \qquad (18)$$

If a parametrization similar to the second term of Eq. (14) is used for $f^0_{B\pi}$, this suggests $\gamma_{B\pi} = 1/\alpha_{B\pi}$ [14]. Interestingly, the fit described above is well consistent with this constraint. Therefore, we will assume this relation in the following.

Our final result for the form factor $f^+_{B\pi}(p^2)$ can then be written in a very convenient form:

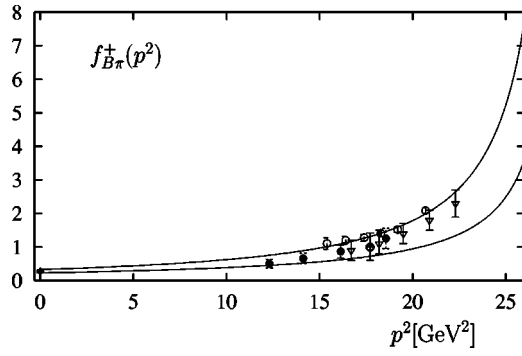$$f^+_{B\pi}(p^2) = \frac{f^+_{B\pi}(0)}{(1 - p^2/m_{B*}^2)(1 - \alpha_{B\pi} p^2/m_{B*}^2)}, \qquad (19)$$

FIG. 2. The LCSR prediction for the $B \to \pi$ form factor in comparison to lattice results. The solid curves indicate the size of the LCSR uncertainties. The lattice results come from FNAL [19] (solid circles), UKQCD [21] (triangles), APE [22] (solid square), JLQCD [23] (open circles), and ELC [19] (semi-solid circle).

where $f_{B\pi}^+(0) = c_B(1 - \alpha_{B\pi})$ has been used, and $f_{B\pi}^+(0)$ and $\alpha_{B\pi}$ are given in Eqs. (7) and (16), respectively. The above parametrization is plotted in Fig. 1. We see that it coincides nicely with the LCSR prediction (4) at low p^2 and approaches the single-pole approximation at large p^2. Figure 1 therefore shows that at small and intermediate momentum transfer our result is actually model independent, the two-pole model (14) being nothing but a convenient parametrization in this region.

Figure 2 shows a comparison of Eq. (19) with recent lattice results [19–23]. The agreement within uncertainties is very satisfactory. Here, the overall uncertainty in the LCSR prediction is estimated by adding the uncertainties from individual sources linearly. This explains why the range of uncertainty updated in Fig. 2 is larger than the uncertainty estimated previously by us and other authors adding the various uncertainties in quadrature. We consider the present procedure to be the appropriate treatment of theoretical uncertainties. Finally, the LCSR prediction also obeys the constraints derived from sum rules for the inclusive semileptonic decay width in the heavy quark limit [24]. This is demonstrated in Fig. 3.

III. THEORETICAL UNCERTAINTIES

The theoretical uncertainties in the LCSRs (4) and (10) originate from uncertainties in the input parameters and from
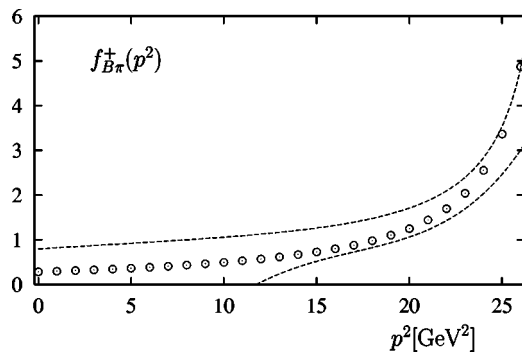

FIG. 3. The LCSR prediction on the form factor $f_{B\pi}^+$ (circles) in comparison to the constraint (dashed lines) derived in Ref. [24].
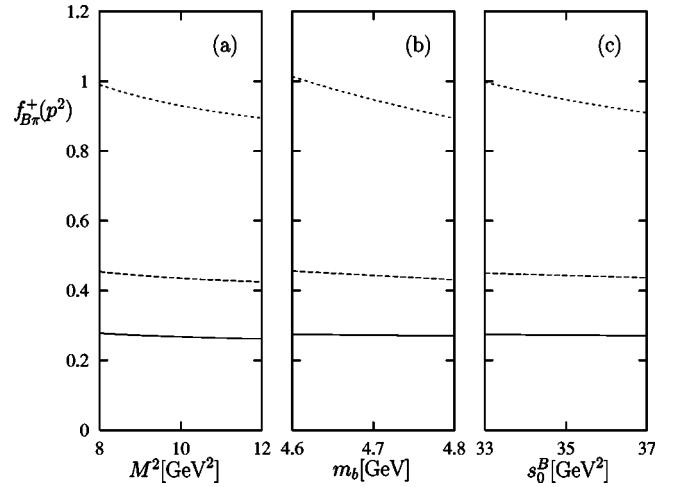

FIG. 4. Sensitivity of the LCSR for $f_{B\pi}^+(p^2)$ on the Borel parameter (a), the b-quark mass (b), and the subtraction threshold (c) at momentum transfer squared $p^2 = 0$ (solid lines), $p^2 = 8$ GeV^2 (long-dashed lines), and $p^2 = 16$ GeV^2 (short-dashed lines).

unknown contributions of higher order in twist and α_s. The former are estimated by varying the numerical values of the input parameters within the ranges given in Sec. II; for the latter we present some plausible arguments concerning the size of these corrections. If not stated otherwise, only a single parameter is varied at a time, while the other parameters are held fixed. For f_B we substitute the corresponding two-point sum rule. The uncertainty in a given quantity is then expressed by plus or minus the interval of variation with respect to the result obtained for the nominal values of the input parameters. Although in the parametrization (19) of $f_{B\pi}^+(p^2)$ the LCSR (4) is only used to determine the normalization at $p^2 = 0$, we investigate the uncertainty of the LCSR prediction (4) in the whole range of validity, that is at $0 \leqslant p^2 < 18$ GeV^2. This serves as a cross-check and ensures the consistency of Eq. (19) with the LCSR (4) in the whole range of overlap. In the region $p^2 > 18$ GeV^2 we rely on the parametrization (19) in a more substantial way. This may introduce some model dependence due to the particular functional form assumed. However, since only the kinematically suppressed region of large momentum transfer is affected, this uncertainty has little influence on the integrated width and the value of V_{ub} extracted from the latter. Our findings are summarized below.

A. Borel mass parameter

The variation of $f_{B\pi}^+$ with M^2 is illustrated in Fig. 4(a). It turns out to be rather small, $\pm(3-5)\%$ depending on p^2. The corresponding variation of $f_{B*}g_{B*B\pi}$ amounts to $\pm 10\%$.

B. b-quark mass and subtraction threshold

Figures 4(b) and 4(c) show the variation of $f_{B\pi}^+$ with m_b and s_0^B, respectively. If m_b and s_0^B are varied simultaneously such that one achieves maximum stability of the sum rule for
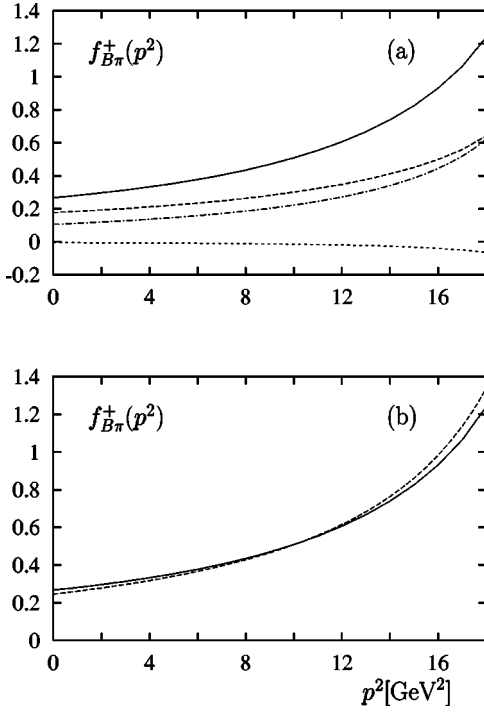
FIG. 5. The LCSR prediction of $f_{B\pi}^+$: (a) individual contributions from twist 2 (dashed line), 3 (dash-dotted line), 4 (dotted line), and the total sum (solid line); (b) with (solid line) and without (dashed line) non-asymptotic corrections to the pion distribution amplitudes.

f_B, the change in $f_{B\pi}^+$ is negligible at small p^2, rising to about $\pm 3\%$ at large p^2. The corresponding variation of $f_{B*}g_{B*B\pi}$ is about $\pm 4\%$.

C. Quark condensate density

The coefficient $\mu_\pi = m_\pi^2/(m_u + m_d)$ of the twist 3 pion distribution amplitude is related to the quark condensate density $\langle \bar{q}q \rangle$ by partial conservation of axial-vector current (PCAC). Therefore, the uncertainty in the quark condensate $\langle \bar{q}q \rangle(\mu_b) = -(268 \pm 10 \text{ MeV})^3$ induces an uncertainty in both the sum rule for f_B and the terms F_0^3 and G_0^3 of the LCSRs (4) and (10), respectively. The resulting uncertainty in $f_{B\pi}^+$ and $f_{B*}g_{B*B\pi}$ is about $\pm 3\%$. Gluon and quark-gluon condensates have little influence on f_B and no direct connection to the LCSR considered here.

D. Higher-twist contributions

No reliable estimates exist for distribution amplitudes beyond twist 4. Therefore, we use the magnitude of the twist 4 contribution to $f_{B\pi}^+$ as an indicator for the uncertainty due to the neglect of higher-twist terms. From Fig. 5(a) we see that the twist 4 term of Eq. (4) contributes less than 2% at low p^2 and about 5% at large p^2 to $f_{B\pi}^+$. Also the twist 4 term in Eq. (10) contributes no more than 5% to $f_{B*}g_{B*B\pi}$.

E. Pion distribution amplitudes

The asymptotic distribution amplitudes and the scale dependence of the nonasymptotic coefficients are determined by perturbative QCD. However, the values of the nonasymptotic coefficients at a certain scale μ_0 are of genuinely nonperturbative origin. They can be determined either from experiment or, eventually, from lattice QCD [25]. For illustration, the twist 2 distribution amplitude appearing in Eqs. (6) and (11) is given by

$$\varphi_\pi(u,\mu) = 6u(1-u)[1 + a_2^\pi(\mu)C_2^{3/2}(2u-1)$$
$$+ a_4^\pi(\mu)C_4^{3/2}(2u-1)], \qquad (20)$$

where $C_n^{3/2}(x)$ are Gegenbauer polynomials, and $a_n^\pi(\mu)$ are the nonasymptotic coefficients. Investigation by means of conformal partial wave expansion justifies the neglect of terms with $n > 4$ (see, e.g., Ref. [26] for further explanation and references).

In Refs. [8,9,11] we have used the Braun-Filyanov (BF) distribution amplitudes [16]. Two recent analyses based on the LCSR for the $\gamma^* \gamma \to \pi^0$ transition form factor [27,28] and the pion form factor [29] indicate that nonasymptotic effects in φ_π are in fact smaller than the effects implied by the original BF coefficients [16]. However, the uncertainties are still sizable. The latter is even more so for the nonasymptotic coefficients of the twist 3 and 4 distribution amplitudes [26]. There is a crude, but simple and as we will see sufficient way to estimate the sensitivity of the LCSRs to nonasymptotic effects, that is by comparing the results obtained with BF and purely asymptotic distribution amplitudes. For $f_{B\pi}^+(p^2)$, this comparison is displayed in Fig. 5(b). We see that the difference is very moderate: about -7% at small p^2 and $+7\%$ at large p^2. The intermediate region around $p^2 = 10 \text{ GeV}^2$ is almost unaffected. A similar investigation of Eq. (10) shows that $f_{B*}g_{B*B\pi}$ increases by about 8% if all nonasymptotic effects are disregarded. Since the LCSR (4) involves convolutions of relatively smooth coefficient functions with normalized distribution amplitudes, the moderate sensitivity to the precise shape of the latter is easy to understand. In contrast, the LCSR (10) depends on the amplitudes at a given point and could, therefore, be strongly affected by nonasymptotic effects. However, in this case the effects have opposite signs for twist 2 and 3, and thus tend to cancel.

F. Perturbative corrections

The NLO QCD corrections to the twist 2 contribution to $f_B f_{B\pi}^+$ derived from Eq. (4) [9,10] amount to about (20–30)%. Corrections of similar size affect the two-point sum rule for f_B [17]. Hence, in the ratio giving $f_{B\pi}^+$ they almost cancel, leaving a net correction of less than 10%. A similar cancellation takes place between the NLO corrections to $f_B f_{B*}g_{B*B\pi}$ derived from Eq. (10) and the NLO corrections to f_B. Here, the net effect is only 5%.

The perturbative corrections to the higher-twist terms are still unknown. Most important are the NLO corrections to $F_0^{(3)}$ and $G_0^{(3)}$. Optimistically, they could be as small as the correction to the quark condensate term in the sum rule for f_B, namely about 2% [30]. More conservatively, they may be of the same order as the twist 2 NLO corrections. Since in LO the twist 3 terms contribute about (30–50)% to the
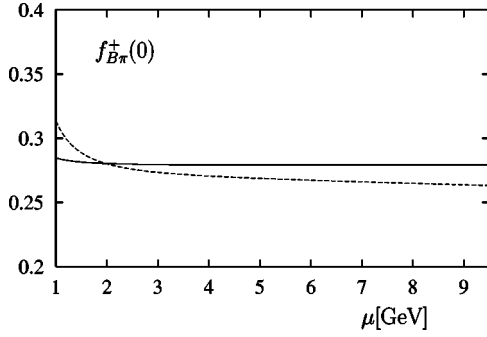
FIG. 6. Scale dependence of the form factor $f_{B\pi}^+(0)$ from LSCRs with f_B calculated from the corresponding μ-dependent two-point sum rule (solid line), and with fixed $f_B = 180$ MeV (dashed line).

LCSR, one may expect corrections to $f_{B\pi}^+$ and $f_{B*}g_{B*B\pi}$ as large as (5–15)% in total. Therefore, it is very important to make every effort to calculate these corrections.

G. Normalization scale

Also the μ dependence of the sum rules for f_B and $f_B f_{B\pi}^+$ turns out to be quite similar. As a result, the ratio of these sum rules yielding $f_{B\pi}^+$ shows very little scale dependence as can be seen from Fig. 6. An analogous cancellation of scale dependences is observed in the ratio of sum rules giving $f_{B*}g_{B*B\pi}$.

The total theoretical uncertainty in Eqs. (4) and (10) is obtained by adding the uncertainties from the different sources given in Secs. III A–III G linearly. However, expecting that the twist 3 NLO corrections will be calculated in near future and assuming that they will turn out to be on the lower side of the range considered in Sec. III F we have not included them in the numerical uncertainty estimates quoted in this paper. The same procedure has been followed in estimating the uncertainty on $\alpha_{B\pi}$ which is given by the ratio of the LCSRs (4) and (10), and has therefore to be studied separately. Finally, in the parametrization (19) of the form factor $f_{B\pi}^+$ the uncertainty in normalization and shape is given by the uncertainty in $f_{B\pi}^+(0)$ and $\alpha_{B\pi}$, respectively.

The theoretical uncertainties quoted in the following section dealing with $D\to\pi$ and $D\to K$ transitions are obtained analogously to the uncertainty on $B\to\pi$.

IV. $D\to\pi$ AND $D\to K$ FORM FACTORS

With the LCSRs (4) and (10) at hand it is straightforward to obtain the corresponding sum rules for the $D\to\pi$ form factor $f_{D\pi}^+$ and for the residue $f_{D*}g_{D*D\pi}/2m_{D*}$ of the $D*$-pole contribution. The input parameters are as follows. For the c-quark pole mass m_c, the subtraction threshold s_0^D, and the factorization scale μ_c we take $m_c = 1.3 \mp 0.1$ GeV, $s_0^D = 6 \pm 1$ GeV^2, and $\mu_c = \sqrt{m_D^2 - m_c^2} \approx 1.3$ GeV. The decay constant f_D is calculated from the two-point QCD sum rule in NLO [17] with the Borel mass squared $M^2 = 1.5 \pm 0.5$ GeV^2 yielding $f_D = 200 \pm 20$ MeV. Again, the variation of the parameters in the above ranges is correlated as indicated by the alternating $\pm$ signs. Furthermore, the pion distribution
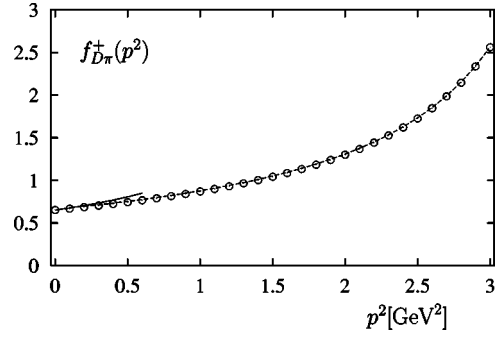

FIG. 7. The $D\to\pi$ form factor: direct LCSR prediction (solid curve), $D*$-pole contribution with the LCSR estimate of the residue (dashed curve), and two-pole parametrization (24) (circles).

amplitudes are to be taken at the scale μ_c. Details can be found in Ref. [15].

The form factor $f_{D\pi}^+$ resulting from Eq. (4) with the input specified above is shown by the solid curve in Fig. 7. For this illustration, we have chosen the nominal values of the parameters. The range of the Borel parameter M^2 in which Eq. (4) satisfies the criteria on the size of the twist 4 terms and the contribution from excited states is found to be $M^2 = 4 \pm 1$ GeV^2. For later use, we also quote the value of $f_{D\pi}^+$ at zero momentum transfer:

$$f_{D\pi}^+(0) = 0.65 \pm 0.11 \tag{21}$$

which nicely agrees with lattice estimates, for example, the world average [20]

$$f_{D\pi}^+(0) = 0.65 \pm 0.10, \tag{22}$$

or the most recent APE result [22], $f_{D\pi}^+(0) = 0.64 \pm 0.05_{-.07}^{+.00}$.

In the case of $D\to\pi$ transitions, the LCSR (4) is reliable as long as $p^2 < m_c^2 - 2m_c\chi \approx 0.6$ GeV^2. Here, the same hadronic scale $\chi \approx 500$ MeV is assumed as for $B\to\pi$. At larger momentum transfer, one may make use of a dispersion relation in analogy to Eq. (13). The residue of the pole contribution from the ground state $D*$ meson can be calculated from the LCSR (10) adjusted to the $D*D\pi$ coupling. One gets

$$f_{D*}g_{D*D\pi} = 2.7 \pm 0.8 \ \text{GeV} \tag{23}$$

with the allowed interval of the Borel parameter being $M^2 = 3 \pm 1$ GeV^2. In Fig. 7, the $D*$-pole contribution is shown by the dashed curve, again for the nominal values of the parameters. Comparison with the LCSR prediction at low p^2 indicates that there is little room for additional contributions from higher resonances, in contrast to what we have found for the $B\to\pi$ transition.

In order to quantify this statement, it is useful to investigate a parametrization of $f_{D\pi}^+(p^2)$ similar to Eq. (19):

$$f_{D\pi}^+(p^2) = \frac{f_{D\pi}^+(0)}{(1 - p^2/m_{D*}^2)(1 - \alpha_{D\pi}p^2/m_{D*}^2)}, \tag{24}$$

PREDICTIONS ON $B \to \pi \bar{l} \nu_l$, $D \to \pi \bar{l} \nu_l$, AND $D \to K \bar{l} \nu_l$ FROM ...

PHYSICAL REVIEW D **62** 114002

where in addition to the D^* pole a second pole is present at the effective mass $m_{D^*}/\sqrt{\alpha_{D\pi}}$. The normalization $f^+_{D\pi}(0)$ is given by Eq. (21) and the deviation in shape from single-pole form is described by the parameter

$$\alpha_{D\pi} = 1 - \frac{2m_{D^*}f^+_{D\pi}(0)}{f_{D^*}g_{D^*D\pi}} = 0.01^{+0.11}_{-0.07}. \qquad (25)$$

The LCSRs (4) and (10) thus predict $\alpha_{D\pi}$ to be consistent with zero, that is complete dominance of the lowest lying D^* pole and negligible influence of higher poles and continuum states. In other words, here the use of the two-pole parametrization (24) does not introduce any significant model dependence. For the nominal values of the parameters, Eq. (24) is plotted in Fig. 7. Comparing this figure with Fig. 1 one clearly sees that the D^* dominance in $f^+_{D\pi}$ is more pronounced than the B^* dominance in $f^+_{B\pi}$. This finding can be understood by considering the splitting between the ground and excited vector meson states in the heavy quark limit, e.g.,

$$\frac{m^2_{D^{*\prime}} - m^2_{D^*}}{m^2_{D^*}} = \frac{2(\Delta' - \Delta)}{m_c} + O(m_c^{-2}), \qquad (26)$$

where we have used the heavy quark mass expansion $m^2_{D^*} = m^2_c + 2m_c\Delta$ and similarly for $m_{D^{*\prime}}$. Since the hadronic scales Δ and Δ' are independent of the heavy quark mass, the relative splitting of the states in the D^* system is expected to be larger than the splitting in the B^* system. Consequently, the heavier B^* states are expected to contribute more to the dispersion relation (13) for $f^+_{B\pi}(p^2)$ than the excited D^* states to the corresponding dispersion relation for $f^+_{D\pi}(p^2)$.

The theoretical uncertainties in Eq. (21) and (23) are estimated analogously to the uncertainties in the B-meson case explained in Sec. III. However, there are certain differences which should be pointed out. First, unlike in $B \to \pi$, the twist 3 term yields the largest individual contribution to $f^+_{D\pi}(p^2)$ as shown in Fig. 8(a). This causes no problem for the light-cone expansion itself because even and odd twists are associated with different chiral structures of the underlying correlation function. The corresponding series are, therefore, independent from each other. More definitely, the expansion of the term in the heavy quark propagator proportional to the quark mass gives rise to a series in even twist, whereas the term proportional to the quark momentum is expanded in a series of terms carrying odd twist. Important for the convergence of the expansion is the observation that the twist 4 contribution is heavily suppressed with respect to the twist 2 contribution as shown in Fig. 8(a). Unfortunately, very little is known about the twist 5 term. If twist 5 is similarly suppressed with respect to twist 3 as twist 4 is suppressed with respect to twist 2, the uncertainty due to the neglected higher-twist contributions is practically negligible. This assumption is made tacitly in all LCSR calculations. Second, the uncertainties in the nonasymptotic coefficients of the pion distribution amplitudes induce an almost momentum-
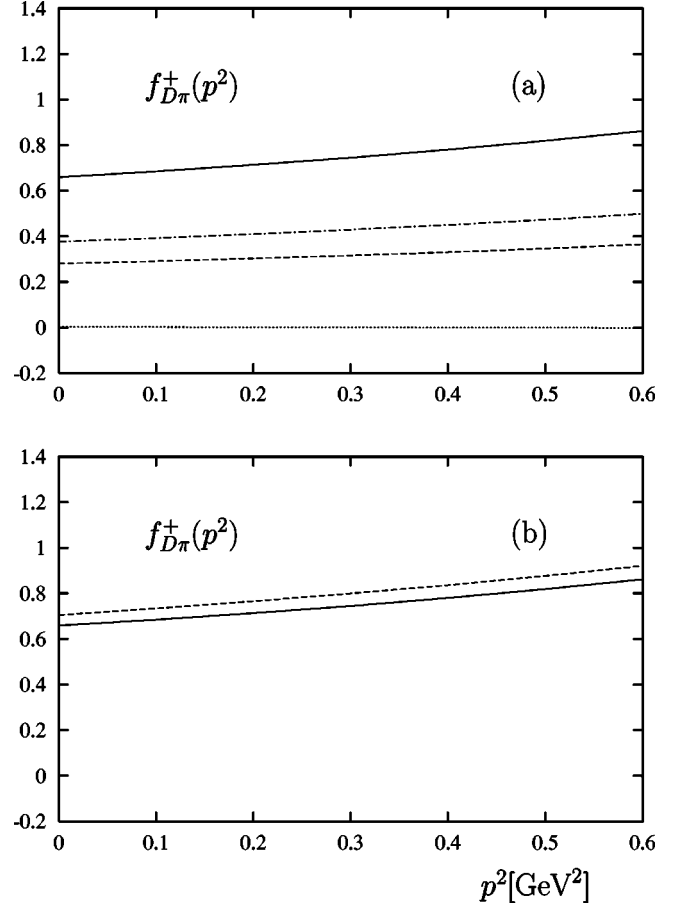

FIG. 8. The LCSR prediction on $f^+_{D\pi}$: (a) individual contributions from twist 2 (dashed line), 3 (dash-dotted line), 4 (dotted line), and the total sum (solid line); (b) with (solid line) and without (dashed line) non-asymptotic corrections to the pion distribution amplitudes.

independent uncertainty in the form factor $f^+_{D\pi}$ by about 5% in contrast to the shape-dependent uncertainty in $f^+_{B\pi}$. This can be clearly seen by comparing Fig. 8(b) and Fig. 5(b). Third, for $D \to \pi$ the NLO QCD corrections to the LCSR at twist 2 tend to be smaller than the corrections to the LCSR for $B \to \pi$, in contradiction to naive expectation. The reason is that the shrinkage of $\alpha_s(m_Q)$ when going from charm to bottom is over-compensated for by the growth of logarithms of the heavy quark mass appearing in the coefficient functions of the sum rules [11]. Quantitatively, the NLO effects on f_D, $f^+_{D\pi}$ and $f_{D^*}g_{D^*D\pi}$ amount to about 10%, in contrast to (20–30)% corrections in the B-meson case. We also expect this tendency to persist for the missing NLO corrections at twist 3. The maximal 15% estimated for $B \to \pi$ would then correspond to about 6% for $D \to \pi$.

The $D \to K$ transition form factor is calculated from the LCSRs (4) and (10) using the same input parameters as for $D \to \pi$ with the exception of the distribution amplitudes. For the kaon distribution amplitude of twist 2 we take

$$\varphi_K(u,\mu) = 6u(1-u)\left[1 + \sum_{n=1}^{4} a^K_n(\mu)C^{3/2}_n(2u-1)\right] \qquad (27)$$

TABLE I. $D \to K$ transition parameters as a function of the s-quark mass.

$m_s(\mu_c)$ (MeV)	100	150	200
$f_{DK}^+(0)$	0.99 ± 0.11	0.78 ± 0.11	0.68 ± 0.09
$f_{D_s^*} g_{D_s^* DK}$	3.9 ± 0.8	3.1 ± 0.6	2.7 ± 0.5
α_{DK}	$-0.08_{-0.07}^{+0.15}$	$-0.07_{-0.07}^{+0.15}$	$-0.06_{-0.07}^{+0.14}$

with $a_1^K(\mu_c) = 0.17$, $a_2^K(\mu_c) = 0.21$, $a_3^K(\mu_c) = 0.07$, and $a_4^K(\mu_c) = 0.08$. In addition to the features of the pion distribution amplitude $\varphi_\pi(u, \mu)$ given in Eq. (20), the above amplitude incorporates effects from $SU(3)$-flavor violation. This is seen from the presence of the coefficients $a_{1,3}$ giving rise to asymmetric momentum distributions for the strange and nonstrange quark constituents inside the kaon. The distribution amplitude φ_K used in Ref. [12] to calculate the $B \to K$ transition form factor differs from Eq. (27) in neglecting $a_{3,4}^K$ which, however, is quantitatively not important. Other $SU(3)$-breaking effects in the distribution amplitudes are neglected. This is certainly justified for the nonasymptotic terms of twist 3 and 4 analyzed recently in Ref. [26] which have anyway only a minor influence on the LCSR as pointed out earlier. For a similar reason, the twist 3 and 4 quark-gluon distribution amplitudes are also taken in the $SU(3)$ limit. Furthermore, in the coefficients of the twist 2 and 3 distribution amplitudes f_π is replaced by $f_K = 160$ MeV, and μ_π by $\mu_K = m_K^2/(m_s + m_{u,d})$, respectively. The latter brings the mass of the strange quark into the game which is not very well known. In Ref. [26] it was advocated to rely on chiral perturbation theory in the $SU(3)$ limit and use

$$\mu_K = \mu_\pi = -2 \frac{\langle \bar{q} q \rangle}{f_\pi^2}. \tag{28}$$

With the quark condensate $\langle \bar{q} q \rangle (1 \text{ GeV}) = -(240 \pm 10 \text{ MeV})^3$, this yields $m_s(1 \text{ GeV}) = 150 \pm 20$ MeV. In the following, we take $m_s(\mu_c) = 150 \pm 50$ MeV which covers the range of most estimates including the rather low mass suggested by some of the lattice calculations [31].

The numerical predictions derived from the LCSRs (4) and (10) with the above input are tabulated in Table I for three different values of the strange quark mass. Figure 9 shows the form factor f_{DK}^+ at $p^2 < 0.6$ GeV^2 and the pole contribution from the D_s^* ground state as a function of the momentum transfer squared. The two-pole parametrization analogous to Eq. (24),

$$f_{DK}^+(p^2) = \frac{f_{DK}^+(0)}{(1 - p^2/m_{D_s^*}^2)(1 - \alpha_{DK} p^2/m_{D_s^*}^2)}, \tag{29}$$

is also displayed in Fig. 9. For these plots we have chosen the nominal values of the input parameters. Whereas the normalization of f_{DK}^+ is rather sensitive to m_s [7], the shape parameter α_{DK} is more or less m_s independent. Moreover, similarly as in the case of $f_{D\pi}^+$, α_{DK} is consistent with zero, implying a strong dominance of the D_s^* pole.
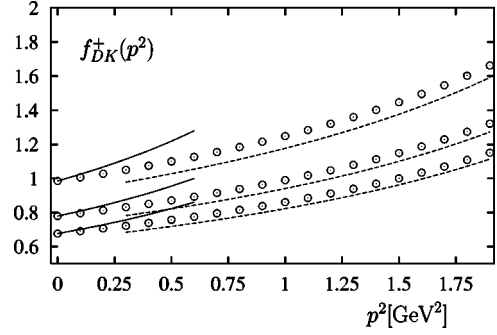

FIG. 9. The $D \to K$ form factor: direct LCSR prediction (solid curve), D_s^*-pole contribution with the LCSR estimate of the residue (dashed curve), and two-pole parametrization (29) (circles). Results are shown for $m_s = 100$ MeV (upper part), 150 MeV (middle part) and 200 MeV (lower part).

This is confirmed by measurements of $D \to K l^+ \nu$ in the CLEO [32] and E687 [33] experiments. The data including those from earlier experiments are summarized in Ref. [34]. For illustration, fitting the single-pole formula

$$f_{DK}^+(p^2) = \frac{f^+(0)}{1 - p^2/M^2} \tag{30}$$

to the world average of the data one obtains

$$f^+(0) = 0.76 \pm 0.03, \quad M = 2.00 \pm 0.15 \text{ GeV}. \tag{31}$$

While for $m_s \approx 150$ MeV the expectation on $f^+(0)$ and the experimental result perfectly match, the mass of the pole is measured to be slightly lighter than $m_{D_s^*} = 2.11$ GeV, but within error it is still consistent with expectation.

There are also lattice determinations of the $D \to K$ form factor which confirm the D^*-pole dominance. The world average of $f_{DK}^+(0)$ is given by [20]

$$f_{DK}^+(0) = 0.73 \pm 0.07, \tag{32}$$

while a more recent calculation by the APE Collaboration [22] yields $f_{DK}^+(0) = 0.71 \pm 0.03_{-0.07}^{+0.00}$. Comparison of these results with Table I implies an s-quark mass which is even somewhat heavier than 150 MeV. While such a value is in accordance with the PCAC expectation (28), it remains to be seen if it can be reconciled with the smallest mass values resulting from lattice investigations [31].

V. SEMILEPTONIC DECAY DISTRIBUTIONS AND WIDTHS

The parametrizations (19), (24) and (29) of the form factors $f_{B\pi}^+$, $f_{D\pi}^+$ and f_{DK}^+ can be used to calculate the distributions of the momentum transfer squared p^2 in exclusive, semileptonic B and D decays, respectively. For $B \to \pi l \bar{\nu}_l$ with $l = e, \mu$ one has
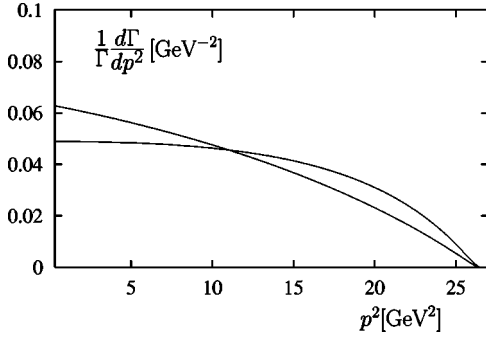
FIG. 10. The normalized distribution of the momentum transfer squared in $B\to\pi\bar{l}\nu_l$ ($l=e,\mu$). The steeper distribution corresponds to $\alpha_{B\pi}=0.25$, the flatter to $\alpha_{B\pi}=0.53$.

$$\frac{d\Gamma(B\to\pi\bar{l}\nu_l)}{dp^2}=\frac{G^2|V_{ub}|^2}{24\pi^3}(E_\pi^2-m_\pi^2)^{3/2}[f_{B\pi}^+(p^2)]^2$$

(33)

with $E_\pi=(m_B^2+m_\pi^2-p^2)/2m_B$ being the pion energy in the B rest frame. The charged lepton is considered massless. Substituting Eq. (19) for $f_{B\pi}^+(p^2)$ one obtains the integrated width

$$\Gamma(B\to\pi\bar{l}\nu_l)=\int_0^{(m_B-m_\pi)^2}dp^2\frac{d\Gamma(B\to\pi\bar{l}\nu_l)}{dp^2}$$

$$=(7.3\pm2.5)|V_{ub}|^2\ \text{ps}^{-1}.$$

(34)

It is important to note that the theoretical uncertainty in the above mainly comes from the uncertainty in the normalization parameter $f_{B\pi}^+(0)$. The uncertainty in the shape parameter $\alpha_{B\pi}$ has very little influence on the integrated width, and so does the use of the two-pole parametrization (19). This is anticipated from the normalized decay distribution plotted in Fig. 10. Our result agrees with the integrated semileptonic width

$$\Gamma(B\to\pi\bar{l}\nu_l)=8.5^{+3.4}_{-1.5}|V_{ub}|^2\ \text{ps}^{-1}$$

(35)

derived in Ref. [35] from a lattice-constrained parametrization of $f_{B\pi}^+$.

Experimentally, combining the branching ratio $BR(B^0\to\pi^-l^+\nu_l)=(1.8\pm0.6)\times10^{-4}$ with the B^0 lifetime $\tau_{B^0}=1.54\pm0.03$ ps [36], one gets

$$\Gamma(B^0\to\pi^-l^+\nu_l)=(1.17\pm0.39)\times10^{-4}\ \text{ps}^{-1}.$$

(36)

From that and Eq. (34) one can then determine the quark mixing parameter $|V_{ub}|$. The result is

$$|V_{ub}|=(4.0\pm0.7\pm0.7)\times10^{-3}$$

(37)

with the experimental error and theoretical uncertainty given in this order. This value lies within the range of $|V_{ub}|$ quoted by the Particle Data Group [36]:

$$|V_{ub}|=0.002-0.005,$$

(38)

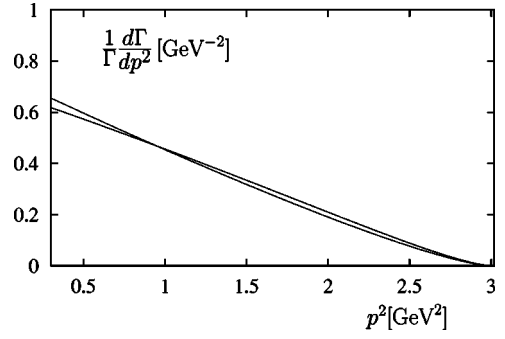FIG. 11. The normalized distribution of the momentum transfer squared in $D\to\pi\bar{l}\nu_l$ ($l=e,\mu$). The steeper distribution corresponds to $\alpha_{D\pi}=-0.06$, the flatter to $\alpha_{D\pi}=0.12$.

and also agrees [15] with the determination from $B\to\rho\bar{l}\nu_l$ [37].

Conversely, turning to $D\to\pi\bar{l}\nu_l$ one can use the known value of $|V_{cd}|$ and subject the LCSR method to an experimental test. From Eq. (24) one obtains

$$\frac{\Gamma(D^0\to\pi^-l^+\nu_l)}{|V_{cd}|^2}=0.13\pm0.05\ \text{ps}^{-1},$$

(39)

while the experimental width following from $BR(D^0\to\pi^-e^+\nu_e)=(3.7\pm0.6)\times10^{-3}$, $\tau_{D^0}=0.415\pm0.004$ ps, and $|V_{cd}|=0.224\pm0.016$ [36] is given by

$$\frac{\Gamma(D^0\to\pi^-e^+\nu_e)}{|V_{cd}|^2}=0.177\pm0.038\ \text{ps}^{-1}.$$

(40)

The agreement is satisfactory, although the theoretical and experimental uncertainties are still too big for a really decisive test. For this reason, it is particularly interesting to note the very small theoretical uncertainties in the normalized momentum distribution shown in Fig. 11. It would be very useful to have comparably precise data.

Similarly for $D\to K\bar{l}\nu_l$, Eq. (29) and Table I yield

$$\frac{\Gamma(D^0\to K^-l^+\nu_l)}{|V_{cs}|^2}$$

$$=\begin{cases}0.151\pm0.058\ \text{ps}^{-1}, & m_s(\mu_c)=100\ \text{MeV},\\0.094\pm0.036\ \text{ps}^{-1}, & m_s(\mu_c)=150\ \text{MeV},\\0.072\pm0.027\ \text{ps}^{-1}, & m_s(\mu_c)=200\ \text{MeV},\end{cases}$$

(41)

which should be compared with the experimental width

$$\frac{\Gamma(D^0\to K^-l^+\nu_l)}{|V_{cs}|^2}=0.087\pm0.004\ \text{ps}^{-1}$$

(42)

derived from $BR(D^0\to K^-l^+\nu)=(3.49\pm0.17)\%$ together with the above D^0 lifetime, and $|V_{cs}|=0.9734-0.9749$ [36]. The latter interval for $|V_{cs}|$ obtained from unitarity of the CKM matrix is very tight and has therefore a negligible influence on the experimental error in Eq. (42). Despite the considerable uncertainty remaining even when m_s is fixed,
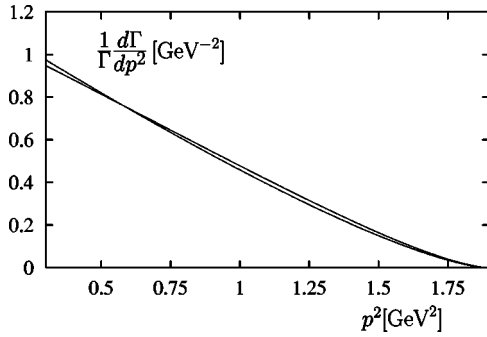
FIG. 12. The normalized distribution of the momentum transfer squared in $D \to K \bar{l} \nu_l$ ($l = e, \mu$). The steeper distribution corresponds to $\alpha_{DK} = -0.14$, the flatter to $\alpha_{DK} = 0.08$.

the comparison of LCSRs and data clearly favors a relatively heavy strange quark mass of about 150 MeV or slightly more. This conclusion is confirmed by considering the ratio of partial widths

$$R = \frac{\Gamma(D^0 \to \pi^- l^+ \nu_l)}{\Gamma(D^0 \to K^- l^+ \nu_l)} = \begin{cases} 0.04, & m_s = 100 \text{ MeV}, \\ 0.07, & m_s = 150 \text{ MeV}, \\ 0.10, & m_s = 200 \text{ MeV}, \end{cases}$$
$$(43)$$

in which the uncertainties not related to the strange quark mass drop out to a large extent. The experimental world average quoted in [34],

$$R = 0.10 \pm 0.02, \qquad (44)$$

again supports a strange quark mass between 150 MeV and 200 MeV. Contrary to the integrated width, the distribution in momentum transfer is insensitive to m_s. Moreover, since the shape parameter α_{DK} is very small or vanishing, the normalized decay distribution in $D \to K \bar{l} \nu_l$ is predicted very reliably as demonstrated in Fig. 12. It can therefore serve as a stringent test similarly as the corresponding distribution in $D \to \pi \bar{l} \nu_l$.

We conclude with a final remark on the uncertainties in the LCSR results. Unlike phenomenological quark models, the LCSR approach allows one to estimate the uncertainty in a given result within the same framework. This is one of the main virtues of QCD sum rules. The model dependence due to the use of a particular two-pole parametrization of the form factors is negligible or unimportant in the present applications. In $B \to pi$ it only concerns the region of large momentum transfer, and is therefore negligible in the integrated semileptonic width and the value of $|V_{ub}|$ extracted from it. The D meson form factors, on the other hand, are

completely dominated by the pole of the respective ground-state vector meson, and therefore insensitive to the effective second pole modeling effects from excited states. In total, the present theoretical uncertainty in the integrated widths of the semileptonic B and D decays considered in this paper is estimated to be about (30–40)%.

Thus, in order to match the accuracy of the data on $D \to \pi \bar{l} \nu_l$ and the precision of $B \to \pi \bar{l} \nu_l$ measurements expected at the new B factories, the theoretical uncertainties have to be reduced by more than a factor of 2. This is not impossible, but will require considerable efforts. Among the most important tasks are the NLO calculation of the twist 3 contributions, a reanalysis of the non-asymptotic corrections to the light-cone distribution amplitudes including mass effects, and an at least rough estimate of the size of the twist 5 terms.

Note added. For completeness, we also present an update of the LCSR prediction on the $B \to K$ transition form factor f_{BK}^+. This form factor plays an important role in the theoretical analysis of the rare decays $B \to K l^+ l^-$, $l = e, \mu, \tau$ [38]. The previous LCSR estimates of f_{BK}^+ [7,12] are restricted to the region of small and intermediate momentum transfer and not applicable to large momentum transfer where the B_s^* pole contribution with the residue given by the $B_s^* BK$ coupling becomes dominant. Here, we have performed an analysis in analogy to the calculation of the $B \to \pi$ form factor described in this paper with the pion distribution amplitudes replaced by the corresponding kaon distribution amplitudes given in Sec. IV. Calculating $f_{BK}^+(0)$ from the LCSR (4) and $f_{B_s^*} g_{B_s^* BK}$ from the LCSR (10), and deriving, from that, the remaining parameter α_{BK} of the two-pole parametrization

$$f_{BK}^+(p^2) = \frac{f_{BK}^+(0)}{(1 - p^2/m_{B_s^*}^2)(1 - \alpha_{BK} p^2/m_{B_s^*}^2)}, \qquad (45)$$

we find $f_{BK}^+(0) = 0.36 \pm 0.07 (0.33 \pm 0.06; 0.41 \pm 0.08)$ for $m_s = 150(200;100)$ MeV and $\alpha_{BK} = 0.28_{-0.08}^{+0.29}$. The ground-state mass $m_{B_s^*} = 5.416$ GeV is taken from [36].

ACKNOWLEDGMENTS

[1] CLEO Collaboration, J. P. Alexander *et al.*, Phys. Rev. Lett. **77**, 5000 (1996).

[2] I. I. Balitsky, V. M. Braun, and A. V. Kolesnichenko, Nucl. Phys. **B312**, 509 (1989); V. M. Braun and I. E. Filyanov, Z.

Phys. C **44**, 157 (1989); V. L. Chernyak and I. R. Zhitnitsky, Nucl. Phys. **B345**, 137 (1990).

[3] G. P. Lepage and S. J. Brodsky, Phys. Lett. **87B**, 359 (1979); Phys. Rev. D **22**, 2157 (1980).

[4] A. V. Efremov and A. V. Radyushkin, Phys. Lett. **94B**, 245 (1980); Theor. Math. Phys. **42**, 97 (1980).

[5] V. L. Chernyak and A. R. Zhitnitsky, Pis'ma Zh. Éksp. Teor. Fiz. **25**, 544 (1977) [JETP Lett. **25**, 510 (1977)]; Yad. Fiz. **31**, 1053 (1980) [Sov. J. Nucl. Phys. **31**, 544 (1980)]; Phys. Rep. **112**, 173 (1984).

[6] M. A. Shifman, A. I. Vainshtein, and V. I. Zakharov, Nucl. Phys. **B147**, 385 (1979); **B147**, 448 (1979).

[7] V. M. Belyaev, A. Khodjamirian, and R. Rückl, Z. Phys. C **60**, 349 (1993).

[8] V. M. Belyaev, V. M. Braun, A. Khodjamirian, and R. Rückl, Phys. Rev. D **51**, 6177 (1995).

[9] A. Khodjamirian, R. Rückl, S. Weinzierl, and O. Yakovlev, Phys. Lett. B **410**, 275 (1997).

[10] E. Bagan, P. Ball, and V. M. Braun, Phys. Lett. B **417**, 154 (1998).

[11] A. Khodjamirian, R. Rückl, S. Weinzierl, and O. Yakovlev, Phys. Lett. B **457**, 245 (1999).

[12] P. Ball, J. High Energy Phys. **809**, 005 (1998).

[13] P. Ball, V. M. Braun, and H. G. Dosch, Phys. Rev. D **44**, 3567 (1991).

[14] D. Becirevic and A. B. Kaidalov, Phys. Lett. B **478**, 417 (2000).

[15] A. Khodjamirian and R. Rückl, in *Heavy Flavours II*, edited by A. J. Buras and M. Lindner (World Scientific, Singapore, 1998), hep-ph/9801443, p. 345.

[16] V. M. Braun and I. E. Filyanov, Z. Phys. C **44**, 157 (1989).

[17] T. M. Aliev and V. L. Eletsky, Yad. Fiz. **38**, 1537 (1983) [Sov. J. Nucl. Phys. **38**, 936 (1983)].

[18] J. Charles, A. Le Yaouanc, L. Oliver, O. Pene, and J. C. Raynal, Phys. Rev. D **60**, 014001 (1999).

[19] J. M. Flynn, in *Proceedings of 28th ICHEP*, Warsaw, 1996, edited by Z. Ajduk and A. K. Wroblewski (World Scientific, Singapore, 1996), hep-lat/9611016, p. 335.

[20] J. M. Flynn and C. T. Sachrajda, in *Heavy Flavours II* [15], hep-lat/9710057, p. 402.

[21] UKQCD Collaboration, K. C. Bowler *et al.*, Phys. Lett. B **486**, 111 (2000).

[22] APE Collaboration, A. Abada *et al.*, Nucl. Phys. B (Proc. Suppl.) **83**, 268 (2000).

[23] JLQCD Collaboration, S. Hashimoto *et al.*, Phys. Rev. D **58**, 014502 (1998).

[24] C. G. Boyd and I. Z. Rothstein, Phys. Lett. B **420**, 350 (1998).

[25] U. Aglietti, M. Ciuchini, G. Corbo, E. Franco, G. Martinelli, and L. Silvestrini, Phys. Lett. B **141**, 371 (1998).

[26] P. Ball, J. High Energy Phys. **01**, 010 (1999).

[27] A. Khodjamirian, Eur. Phys. J. C **6**, 477 (1999).

[28] A. Schmedding and O. Yakovlev, Phys. Rev. D (to be published), hep-ph/9905392.

[29] V. M. Braun, A. Khodjamirian, and M. Maul, Phys. Rev. D **61**, 073004 (2000).

[30] M. Neubert, Phys. Rev. D **45**, 2451 (1992).

[31] S. Ryan, hep-ph/9908386.

[32] CLEO Collaboration, A. Bean *et al.*, Phys. Lett. B **317**, 647 (1993).

[33] E687 Collaboration, P. L. Frabetti *et al.*, Phys. Lett. B **364**, 127 (1995).

[34] ''The BaBar Physics Book,'' edited by P. F. Harrison and H. R. Quinn, Report No. SLAC-R-504, 1998, Chap. 12.

[35] UKQCD Collaboration, L. Del Debbio, J. M. Flynn, L. Lellouch, and J. Nieves, Phys. Lett. B **416**, 392 (1998).

[36] Particle Data Group, C. Caso *et al.*, Eur. Phys. J. C **3**, 1 (1998); and 1999 off-year partial update for the 2000 edition available on the PDG WWW pages (URL: http://pdg.lbl.gov/).

[37] P. Ball and V. M. Braun, Phys. Rev. D **55**, 5561 (1997); **58**, 094016 (1998).

[38] A. Ali, P. Ball, L. T. Handoko, and G. Hiller, Phys. Rev. D **61**, 074024 (2000).